Materials Transactions, Vol. 56, No. 7 (2015) pp. 928 to 932
Special Issue on Long-Period Stacking Ordered Structure and Its Related Materials II

Three-Dimensional Shapes and Distributions of Long-Period Stacking Ordered Structures in $Mg_{97}Zn_1Gd_2$ Cast Alloys Characterized by Electron Tomography

Kazuhisa Sato[1,*], Shuhei Matsunaga[2], Shunya Tashiro[2], Yohei Yamaguchi[2], Takanori Kiguchi[1] and Toyohiko J. Konno[1]

[1]*Institute for Materials Research, Tohoku University, Sendai 980-8577, Japan*
[2]*Depertment of Materials Science, Tohoku University, Sendai 980-8579, Japan*

Three-dimensional (3D) configurations of 14H long-period stacking ordered (LPSO) structures formed in $Mg_{97}Zn_1Gd_2$ cast alloys at intermediate stages of the formation process have been studied by single tilt-axis electron tomography using high-angle annular dark-field scanning transmission electron microscopy. Lateral morphology of the 14H LPSO is clearly visualized by reconstructing 3D volumes. An existence of "dent-shaped" area was found in a 3D reconstructed volume for the first time. The edge of LPSO shows a characteristic triangular shape with an angle of 60°, which indicates that the growth front is parallel to $\{11\bar{2}0\}_{Mg}$. It is suggested that in-plane irregular or characteristic shapes are related to the lateral growth mechanism of LPSO. Electron tomography has proven to be an indispensable tool to characterize in-plane structural information of LPSO formed in α-Mg matrix. [doi:10.2320/matertrans.MH201406]

(Received January 26, 2015; Accepted March 13, 2015; Published May 8, 2015)

Keywords: *long-period stacking ordered (LPSO), magnesium-zinc-gadolinium, electron tomography, lateral morphology, lateral growth, scanning transmission electron microscopy (STEM)*

1. Introduction

Magnesium alloys containing transition metal (TM) together with rare earth (RE) elements such as Mg-Zn-Y have been attracting much interest as next generation lightweight structural materials due to their properties such as low density, high specific strength, damping capacity, recycling efficiency, and so on. The strength of the materials can be attributed to the characteristic long-period stacking ordered (LPSO) structure (synchronized LPSO) formed in α-Mg matrix.[1)] In spite of the technical importance, the formation mechanism of the synchronized LPSO has not been clarified yet. Recent structural characterization of the LPSO relies on scanning transmission electron microscopy (STEM) with an improved resolution and chemical sensitivity. The state-of-the-art electron imaging techniques enable atomic scale characterization of structural and chemical irregularities in the LPSO.[2–4)] However, the images obtained by this technique are projections of three-dimensional (3D) objects; and in order to better understand the nature of the formation behavior of LPSO, visualization of 3D structures is greatly needed. In this respect, electron tomography has opened a new prospect: the technique can retrieve 3D structural information usually missing in (S)TEM.[5)]

The Mg-Zn-RE alloys can be classified into two categories from the viewpoints of formation processes of the LPSO.[6)] The alloys that can give rise to LPSO structures in an as-cast state are termed as type I, and the aforementioned Mg-Zn-Y alloy is representative of this type. For example, in a Mg-0.7 at%Zn-1.4 at%Y alloy, LPSO structures remain along grain boundaries and as particles inside the matrix even after solution treatment at 793 K.[7)] On the other hand, those where LPSO do not form in as-cast state are so called type II alloy. For example, the Mg-Zn-Gd system belongs to this category.[8)] In this alloy system, no LPSO phase exists in the as-cast state and the 14H-type LPSO is formed by aging at temperatures higher than 623 K. Hence the type II alloy is suitable for investigating growth process of the LPSO as a function of annealing temperature and time.

In this study we have hence chosen to characterize 3D structures of the LPSO formed in $Mg_{97}Zn_1Gd_2$ alloys at intermediate stages of LPSO formation by means of single tilt-axis tomography using high-angle annular dark-field (HAADF) STEM.

2. Experimental Procedure

The Mg-Zn-Gd cast alloy ingots were prepared using high-frequency induction heating in an Ar atmosphere. The nominal composition of the alloy is $Mg_{97}Zn_1Gd_2$ (at%). We confirmed that the as-cast alloy is composed of α-Mg matrix (solid solution phase) and a secondary phase as reported in the literature.[8)] The specimens were then annealed at 773 K in the Ar atmosphere for different intervals of 0.06, 0.9 and 18 ks, and then quenched into ice water. Here, the aging temperature was selected based on the time-temperature-transformation (TTT) diagram reported by Yamasaki *et al.*[8)] To prepare samples for TEM, disk-shaped specimens were mechanically thinned followed by Ar ion milling. Details of the TEM specimen preparation can be found in the literature.[4)]

Microstructures of the alloy were characterized using an FEI TITAN^3 60-300 STEM operating at 300 kV with a CEOS aberration (C_S) corrector for the probe-forming lens. Tilt-series of HAADF-STEM images were obtained sequentially from 0° to −70° and then 0° to +70° with the tilt angle increment of 2° using a single-axis tilt holder (Fischione model 2020). We set the electron probe convergence to be 10–14 mrad in semi-angle, taking into account a short focal length of the C_S-corrected STEM. Inner collection angle on the HAADF-detector was set to be 50 mrad. We employed simultaneous iterative reconstruction technique (SIRT) and weighted back-projection (WBP) method for 3D reconstruction of the obtained tilt-series dataset after tilt-axis alignment.

*Corresponding author, E-mail: ksato@imr.tohoku.ac.jp

3. Results and Discussion

Evolution of the microstructure was monitored by electron diffraction and HAADF-STEM imaging as a function of aging time at 773 K. In the as-cast alloy no LPSO phase was detected as mentioned above. Formation of solute-segregated stacking faults (SFs)[8] was detected by electron diffraction as an emergence of weak streaks between fundamental reflections in the $[0001]^*_{Mg}$ direction after aging for 0.06 ks. The streaks split into six spots after aging for 0.9 ks; these satellite reflections indicate the formation of the 14H LPSO structure. At this stage the LPSO appears as thin bands with a thickness less than 20 nm in the $[0001]_{Mg}$ direction. After aging for 18 ks, the LPSO bands have grown in the $[0001]_{Mg}$ direction, typically ~30 nm in thick, and some of then reached as thick as 200 nm.

Figure 1(a) shows a HAADF-STEM image and a selected area electron diffraction (SAED) pattern of a specimen after aging at 773 K for 18 ks. The beam incidence is in the $[\bar{1}2\bar{1}0]_{Mg}$ direction. Distribution of different sized LPSO is clearly seen as bright straight bands/lines that appear as atomic number (Z) contrasts. In this area, most of the LPSO is thinner than 30 nm, indicating intermediate stage of LPSO formation. Thin bands less than 10 nm can be classified as solute-segregated SFs. Small particulate precipitates dispersed in the central part of the image other than LPSO are the residual secondary phase of $(Mg, Zn)_3Gd$ as reported in the literature.[9] Figure 1(b) shows a HAADF-STEM image observed at a high tilt angle of 60°. Tilt axis is in the horizontal direction of this image. Overlapping of plate-like LPSO and their lateral features are seen in this image, viewed from an oblique direction with respect of the thin TEM specimen.

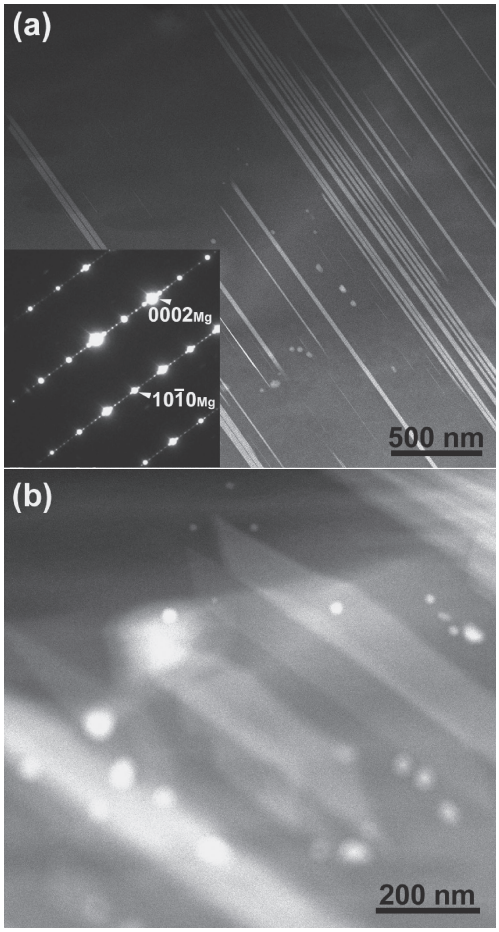

Fig. 1 (a) HAADF-STEM image and SAED pattern of a $Mg_{97}Zn_1Gd_2$ cast alloy after aging at 773 K for 18 ks. The beam incidence is parallel to $[\bar{1}2\bar{1}0]_{Mg}$. (b) HAADF-STEM image observed at a high tilt angle of 60°. Tilt axis is in the horizontal direction of the image.

To elucidate 3D distributions of the LPSO structures at an intermediate stage of their formation process, we have carried out electron tomography for specimens after aging at 773 K for 18 ks. Figure 2 shows snapshots of reconstructed 3D images viewed from several directions. Tilt axis is in the vertical direction of the images. The 3D structures were reconstructed by SIRT using a tilt-series dataset after the tilt-axis alignment. Note that we employed images taken at tilt angles between −62° and +62° for 3D reconstruction based on careful inspection of contrasts. The reconstructed volume is 1961 nm × 2408 nm × 1320 nm (456 pixels × 560 pixels × 307 pixels) with the pixel size of 4.3 nm/pixel. As can be seen, 3D configurations of the LPSO and residual particulate precipitates are clearly reconstructed. It should be noted that lateral width of the LPSO exceeds the foil thickness in the observed area. Lateral morphology is also visualized by rotating the reconstructed 3D volume. It is also noted that edge of each LPSO band has characteristic triangular shapes.

Figure 3(a) shows another example of a HAADF-STEM image of thin LPSO structures. The beam incidence is close to $[\bar{1}2\bar{1}0]_{Mg}$. Distribution of thin LPSO structures, as appear as straight lines by Z-contrast, is clearly seen. Formation of 14H LPSO structures was confirmed by electron diffraction, which showed satellite peaks due to the long-period stacking. Note that the LPSO grows on a plane parallel to $(0001)_{Mg}$. The rectangular area surrounded by broken lines was then selected and reconstructed by SIRT after tilt-axis correction. The axis of tilting is in the vertical direction in this image. Figure 3(b) shows a snapshot of the reconstructed volume by SIRT, which corresponds to the 2D image shown in Fig. 3(a). We employed images taken at tilt angles between −70° and 56° for 3D reconstruction. The reconstructed volume is 7212 nm × 8978 nm × 2710 nm (591 pixels × 742 pixels × 224 pixels) with a pixel size of 12.1 nm. Thickness of the reconstructed area was found to be approximately 1.2 μm. It should be mentioned that at the tilt angle of 70° the specimen thickness reaches 3.5 μm; the thickness is still within the maximum observable limit for electrons accelerated at 300 kV.[10,11] As seen, shapes and distribution of the LPSO are well reproduced. Another snapshot shown in Fig. 3(c), viewed from an oblique direction, revealed an existence of an in-plane "dent-shaped" area of the LPSO as marked by a double-arrowhead, which has not been reported so far. The "dent-shaped" area corresponds to the area in Fig. 3(a) as marked by a double-arrowhead, where the intensity of the Z-contrast viewed from the edge-on direction is markedly reduced due to a reduction of lateral width of LPSO in $[\bar{1}2\bar{1}0]_{Mg}$ direction. This result clearly indicates that a decrease in Z-contrast of LPSO is not always caused by variation of chemical composition of solute elements. Observation frequency of the "dent-shaped" area was 20% in

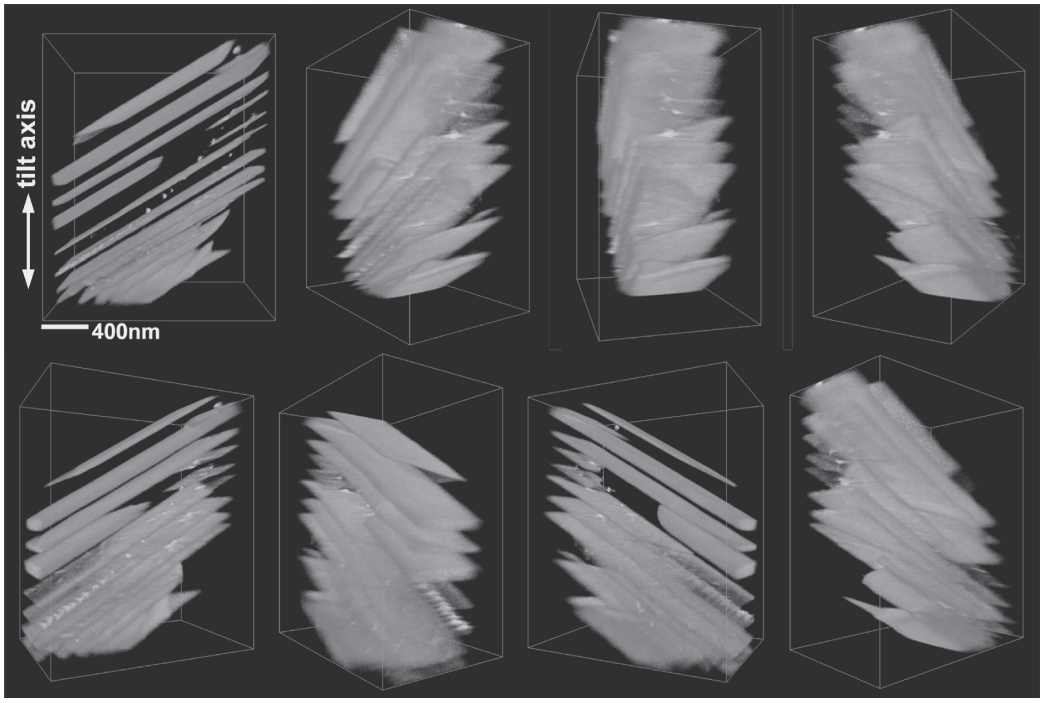

Fig. 2 Reconstructed 3D volumes of a $Mg_{97}Zn_1Gd_2$ cast alloy after aging at 773 K for 18 ks. The reconstructed volume is 1961 nm × 2408 nm × 1320 nm with the pixel size of 4.3 nm/pixel.

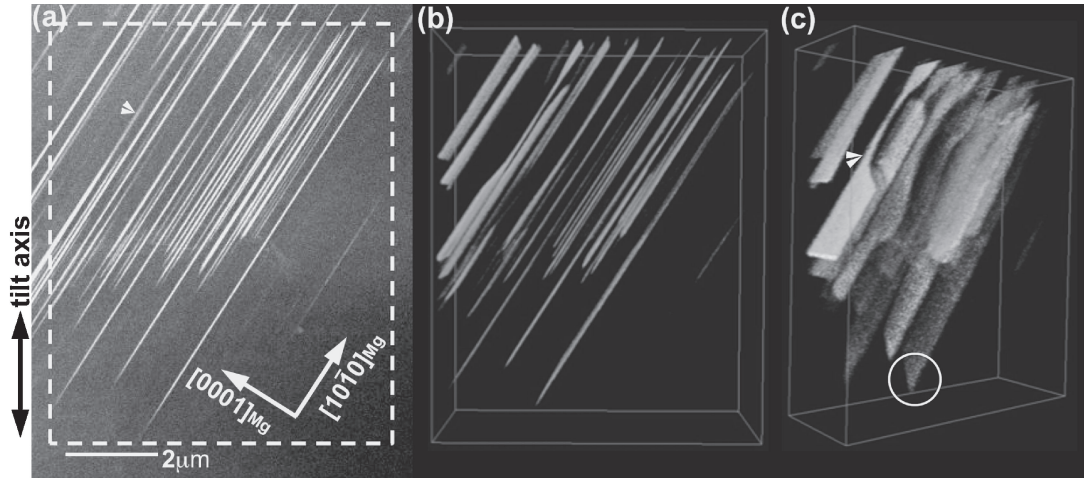

Fig. 3 (a) HAADF-STEM image of a $Mg_{97}Zn_1Gd_2$ cast alloy after aging at 773 K for 18 ks. The observed area is composed of thin LPSO bands. (b) A snapshot of 3D reconstructed volume corresponds to the area shown in Fig. 3(a). The reconstructed volume is 7212 nm × 8978 nm × 2710 nm with a pixel size of 12.1 nm. (c) An oblique view of the 3D reconstructed volume, rotated by 40° from the view shown in Fig. 3(b) with respect to the tilt axis.

the reconstructed volume shown in Fig. 3 (LPSOs including the "dent-shaped" area was 5 out of 25 LPSOs). It should be mentioned that the present result may contain approximately 12% of error in z-direction parallel to optical axis due to the missing wedge, which is introduced by a limited maximum tilt angle.[12] Here, also note that a characteristic triangular shape can be seen at the edge of an LPSO band as marked by a circle. Although the detailed growth mechanism of the LPSO is not clear, it is presumed that such irregular or characteristic shapes are related to the lateral growth mechanism of the LPSO.

Figure 4(a) shows a HAADF-STEM image of an area with sparsely distributed thin LPSO plates. Some of the thin plates are solute-segregated SFs rather than LPSO. We selected a rectangular area surrounded by the solid lines for 3D reconstruction. The axis of tilting is in the vertical direction in this image. The result reconstructed by WBP method is shown in Fig. 4(b). For this dataset, WBP gives a better result in reconstruction of thin plates than SIRT does (a similar result was obtained in our previous study on nanoparticles[13]). The reconstructed volume is 366 nm × 1574 nm × 241 nm (85 pixels × 366 pixels × 56 pixels) with the pixel size of 4.3 nm. The maximum tilt angle employed for the reconstruction was 60°. In this area there are three very fine LPSO plates (and/or solute-segregated SFs) as indicated by arrowheads; which overlap each other and form a step-like

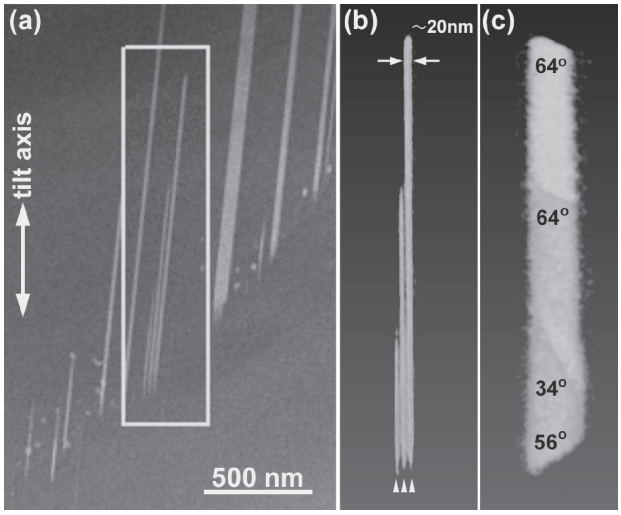

Fig. 4 (a) HAADF-STEM image of a $Mg_{97}Zn_1Gd_2$ cast alloy after aging at 773 K for 18 ks. The observed area is composed of sparsely distributed thin LPSO plates (and/or solute-segregated SFs). The reconstructed volume is 366 nm × 1574 nm × 241 nm with the pixel size of 4.3 nm. (b) A snapshot of 3D reconstructed volume corresponds to the rectangular area shown in Fig. 4(a). (c) Lateral morphology of three overlapped thin plates.

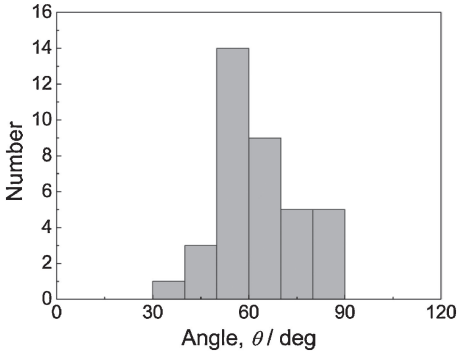

Fig. 5 A histogram of in-plane edge angles of LPSO obtained from a $Mg_{97}Zn_1Gd_2$ cast alloy after aging at 773 K for 18 ks.

structure. Lateral morphology of this area is shown in Fig. 4(c). As can be seen, the edge of each plate shows characteristic triangular shapes with different angles as labeled in the image. In this manner, we measured edge angles of the LPSO plates and made a histogram, which is shown in Fig. 5. This analysis disclosed that the edge angles distribute between 30° and 90°, and angles around 60° are dominant. It is then suggested that these angles are the crystallographic features of LPSO structures, that grow parallel to the (0001) planes of the α-Mg matrix having hexagonal closed packed (hcp) structure.

To clarify the origin of edge angles shown above, we cross-examined the morphological features of LPSO with their crystallography based on the reconstructed 3D volumes and electron diffraction patterns. These examinations led us to propose model structures as shown in Fig. 6. Here, the angle of 60° corresponds to $(11\bar{2}0)_{Mg}$, while the angles of 30° and 90° correspond to $(01\bar{1}0)_{Mg}$ and $(10\bar{1}0)_{Mg}$, respectively. Note that the latter two planes are symmetrically equivalent in the hcp structure. It should be noted that frequent occurrence of edge angles of about 60° implies that

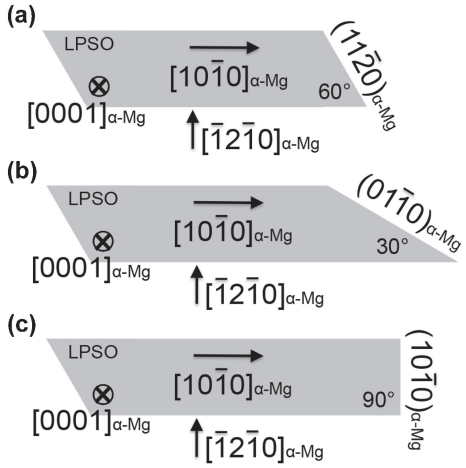

Fig. 6 Schematic models of lateral morphology of LPSO deduced from 3D reconstructed volumes and electron diffraction patterns.

$(11\bar{2}0)_{Mg}$ is a preferable plane for lateral growth of LPSO in α-Mg matrix. Such structural information related to lateral morphology of LPSO has not been obtained except scanning tunneling microscopy[14] and hence the present results demonstrate the usability of electron tomography as a tool to characterize 3D microstructures in medium scale range from nanometer to a few micrometers.

4. Conclusion

We have characterized 3D configurations of 14H LPSO structures formed in $Mg_{97}Zn_1Gd_2$ cast alloys at intermediate stages of LPSO formation by means of single tilt-axis electron tomography using HAADF-STEM. The results can be summarized as follows.

(1) Tilt-series dataset obtained by HAADF-STEM leads to a clear-cut 3D reconstruction of LPSO structures distributed in the α-Mg matrix. Solute-segregated SFs less than 10 nm in thick as well as residual particulate secondary phase are also reproduced in a 3D volume.

(2) Lateral morphology of 14H LPSO structures is clearly visualized by the 3D reconstruction of 2D tilt-series dataset. Existence of an in-plane "dent-shaped" area of the LPSO has been revealed.

(3) Edges of 14H LPSO structures show a characteristic triangular shape with angles between 30° and 90°. The angle of the most frequent appearance is 60°, which corresponds to a growth front parallel to $\{11\bar{2}0\}_{Mg}$, while less frequently emerging angles of 30° and 90° both correspond to $\{10\bar{1}0\}_{Mg}$.

(4) It is suggested that $\{11\bar{2}0\}_{Mg}$ is the preferable plane for lateral growth of LPSO structures.

Acknowledgments

This study is supported by Grant-in-Aid for Scientific Research on Innovative Areas "Synchro-LPSO" (No. 23109006 & 26109702) from the Ministry of Education, Culture, Sports, Science and Technology, Japan. The authors wish to thank Prof. Y. Kawamura and Dr. M. Yamasaki of Kumamoto University for providing us Mg-Zn-Gd alloys,

and Ms. K. Ito for 3D reconstruction. KS acknowledges financial support from the Japan Science Technology Agency "Development of systems and technology for advanced measurement and analysis" program and the Tanikawa Fund Promotion of Thermal Technology.

REFERENCES

1) Y. Kawamura, K. Hayashi, A. Inoue and T. Masumoto: Mater. Trans. **42** (2001) 1172–1176.
2) E. Abe, A. Ono, T. Itoi, M. Yamasaki and Y. Kawamura: Philos. Mag. Lett. **91** (2011) 690–696.
3) H. Yokobayashi, K. Kishida, H. Inui, M. Yamasaki and Y. Kawamura: Acta Mater. **59** (2011) 7287–7299.
4) T. Kiguchi, Y. Ninomiya, K. Shimmi, K. Sato and T. J. Konno: Mater. Trans. **54** (2013) 668–674.
5) P. A. Midgley and M. Weyland: Ultramicrosc. **96** (2003) 413–431.
6) Y. Kawamura and M. Yamasaki: Mater. Trans. **48** (2007) 2986–2992.
7) J. B. Lee, K. Sato, T. J. Konno and K. Hiraga: Mater. Trans. **50** (2009) 222–225.
8) M. Yamasaki, M. Sasaki, M. Nishijima, K. Hiraga and Y. Kawamura: Acta Mater. **55** (2007) 6798–6805.
9) Y. Jono, M. Yamasaki and Y. Kawamura: Mater. Trans. **54** (2013) 703–712.
10) T. Imura: *High Voltage Electron Microscopy*, ed. by P. R. Swann, C. J. Humphreys and M. J. Goringe, (Academic Press, New York, 1974) pp. 179–188.
11) R. Uyeda and M. Nonomiya: Jpn. J. Appl. Phys. **7** (1968) 200–208.
12) N. Kawase, M. Kato, H. Nishioka and H. Jinnai: Ultramicrosc. **107** (2007) 8–15.
13) K. Sato, K. Aoyagi and T. J. Konno: J. Appl. Phys. **107** (2010) 024304.
14) S. Kurokawa, A. Yamaguchi and A. Sakai: Mater. Trans. **54** (2013) 1073–1076.